

# Conductivity and Conjugation Length in Poly(3-methylthiophene) Thin Films

A. Yassar, J. Roncali,\* and F. Garnier

Laboratoire des Matériaux Moléculaires, CNRS, ER 241, 2 rue Henry Dunant, 94320 Thiais, France. Received May 3, 1988; Revised Manuscript Received July 20, 1988

**ABSTRACT:** The evolution of the morphology and electrical conductivity of poly(3-methylthiophene) thin films has been analyzed at various stages of the polymerization reaction. It is shown that the progress of the electropolymerization is accompanied with an increasing morphological disorder and by a steep decrease of the conductivity. Conversely, when the polymer growth is limited to films of a few nanometers thickness, more compact and more ordered materials are obtained while the conductivity increases strongly, reaching values in the range of  $2 \times 10^3 \text{ S cm}^{-1}$ . A parallel analysis of the variation of the electrochemical and spectroscopic properties as a function of film thickness shows that the anodic current peak  $E_p$  shifts nearly 100 mV toward less positive values while the absorption maximum shifts bathochromically ca. 40 nm, confirming that the mean conjugation length is noticeably more extended in ultrathin polymer films. These results show that both the molecular structure and the chains stacking order are subject to an increasing disorder as the polymerization progress.

## Introduction

During the past few years, conducting polymers derived from five-membered heterocycles such as polypyrrole and particularly polythiophene have received increasing attention owing to their improved environmental stability compared to polyacetylene and also because they can be easily prepared as films of controlled thickness by electrochemical synthesis.<sup>1</sup> On the theoretical level, the mechanism of charge transport is still subject to investigation, and it has been shown that the nondegenerate ground state of these polymers leads to polarons and bipolarons states resulting from the coupling of electronic excitations to chain distortions, as the dominant charged species involved in the charge-transport process.<sup>2</sup> On the other hand, these polymers are extensively investigated in view of their potential use as molecular materials in highly specific applications such as modified electrodes and electronic devices.<sup>3,4</sup> Although it seems evident that future developments in these fields are still conditioned by the obtention of polymer films of controlled structure and properties, the problems related to the analysis of the electropolymerization mechanism in relation to the improvement of the electrosynthesis conditions have been seldom considered in the literature. Thus, until recently, discrepancies of several orders of magnitude could be found between the conductivity values reported by different groups.<sup>5</sup> Significant progress in the control of the structure and properties of polythiophenes have been accomplished in recent years, and it has been shown that the conductivity of poly(3-methylthiophene) (PMeT) can reach values in the range of  $500 \text{ S cm}^{-1}$  when operating in optimized electrosynthesis conditions.<sup>6</sup> Furthermore, we have shown that the increase of the conductivity is tightly correlated to an enhancement of the mean conjugation length in the polymer.<sup>6b,7,8</sup>

As a further step in the study of the electropolymerization of thiophene derivatives, we have analyzed the evolution of the morphology and electrical conductivity of PMeT films as a function of their thickness, e.g., of the degree of advancement of the electropolymerization reaction. We show that films of a few nanometers thickness are more compact and noticeably more conductive than thicker films. These observations are completed by a parallel analysis of the electrochemical and spectroscopic properties of the polymer that indicates that the mean conjugation length is more extended in ultrathin films. These two series of results suggest that both the molecular structure and the packing arrangement of the polymer

chains are subject to an increasing disorder as polymerization proceeds.

## Experimental Section

**Film Preparation.** Solvents and reagents were purified according to previously described procedures.<sup>6b</sup> Electrosynthesis were carried out in a one-compartment three-electrode cell containing various concentrations of 3-methylthiophene and 0.02 M  $\text{Bu}_4\text{NPF}_6$  in nitrobenzene. The syntheses were performed in galvanostatic conditions, at ambient temperature under an argon atmosphere. The solutions were degassed by argon bubbling prior to electropolymerization. Indium-tin oxide (ITO,  $80 \Omega \text{ cm}^{-2}$ ) or tin oxide ( $\text{SnO}_2$ ,  $10 \Omega \text{ cm}^{-2}$ ) coated glass electrodes or a polished platinum plate were used as anodes, and aluminum foil or ITO electrodes as cathodes. All potentials refer to a saturated calomel electrode SCE. The films thicknesses were determined from the deposition charge, with the relation  $2 \text{ nm}/(\text{mC cm}^2)$  established from thickness measurements performed on thicker films ( $0.5\text{--}5 \mu\text{m}$ ) using a Sylvac P 100 thickness monitor. For thinner films, the linearity of the optical density of the films vs deposition charge observed over the whole range of thickness confirmed that the polymerization yield is independent of film thickness.

**Conductivity Measurements.** Thin films for conductivity measurements were grown on ITO electrodes of  $5\text{--}6\text{-cm}^2$  area or on a  $8\text{-cm}^2$  platinum plate polished with  $0.05\text{-}\mu\text{m}$  diamond paste and heated to redness in air before each experiment. After polymerization, the films were rinsed with acetone and dried in an argon flow. The films were then covered with adhesive tape and peeled off the electrode. The films were cut in the form of  $2 \times 0.5 \text{ cm}$  strips, and conductivities were measured on the electrode side of the films by a standard four-probe technique using mercury drop contacts. Scanning electron microscopy (SEM) was performed on a Cambridge S 250 scanning electron microscope. Pictures of the electrode side of the films were obtained on films prepared in the above-described conditions, while views of the solution side were taken on films deposited on  $0.4\text{-cm}$ -diameter polished platinum disks and left on the electrodes.

**Electrochemistry.** For electrochemical characterization, the films were synthesized in the above described conditions on  $0.9 \times 2 \text{ cm}$  ITO electrodes. After the synthesis, the films were rinsed with acetonitrile and placed in a three-electrode cell containing 0.1 M anhydrous lithium perchlorate in acetonitrile. Electrosynthesis and cyclic voltammetric experiments were performed with a PAR 175 potentiostat/galvanostat equipped with a PAR 173 universal programmer and a PAR 179 plug-in digital coulometer.

**Visible Absorption Spectroscopy.** The films for absorption spectroscopy have been prepared in similar conditions on  $0.9 \times 2 \text{ cm}$   $\text{SnO}_2$  electrodes, rinsed with acetonitrile, and electrochemically undoped in 0.1 M  $\text{Bu}_4\text{NPF}_6$  in acetonitrile by application of a potential of  $-0.2 \text{ V/SCE}$  until the cathodic current reaches a constant value. Absorption spectra were recorded on a Cary 219 spectrometer.

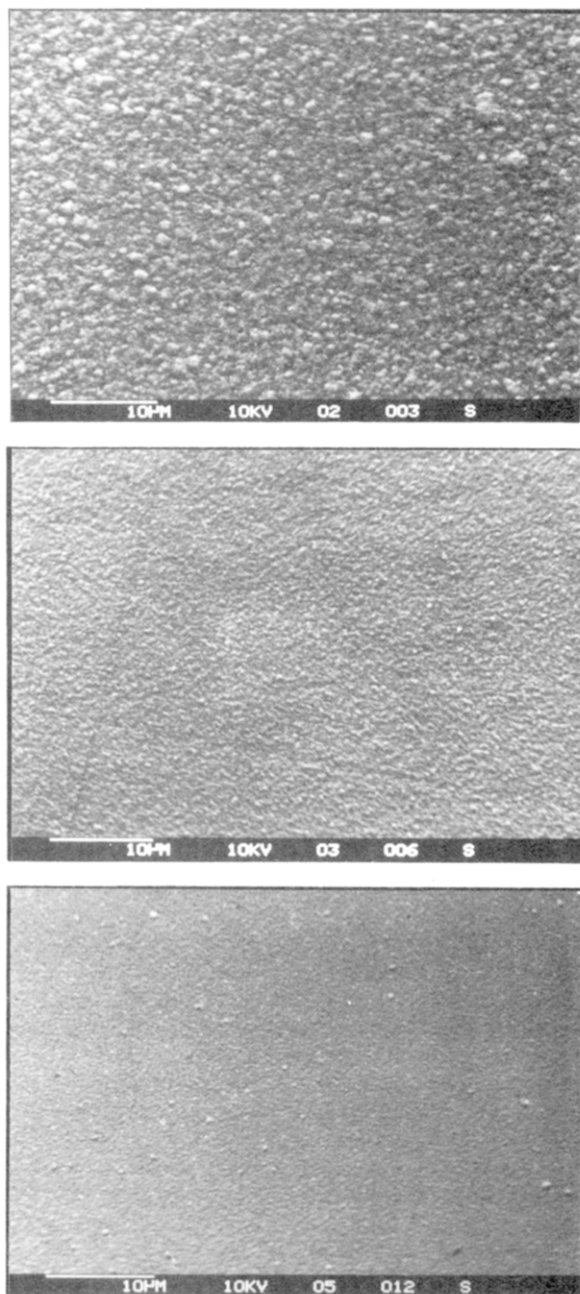


**Figure 1.** SEM pictures at various stages of polymerization of the solution side of PMeT films prepared on 0.13-cm<sup>2</sup> Pt disks with 0.1 M MeT and 4 mA/cm<sup>2</sup>. Film thickness: top, 1000 nm; middle, 200 nm; bottom, 50 nm.

## Results and Discussion

**Effect of Thickness on the Morphology of the Films.** Previous studies on electrogenerated conducting polymers have shown already that the thickness of the polymer film and hence the progress of the polymerization exerts a strong effect on the morphology of the polymer. Thus when the thickness of polypyrrole films exceeds 1–2  $\mu\text{m}$ , the film surface remains no longer smooth but adopts a cauliflower structure constituted of hemispheres of several micrometers diameter.<sup>9</sup> Differences in the morphology of thin and thick films have been also mentioned for polythiophenes,<sup>10</sup> but less data are available. The morphology of PMeT films has been examined by SEM at various stages of the electropolymerization to get more detailed information on this point. Figure 1 shows SEM micrographs of the solution side of PMeT films prepared on Pt disk electrodes with thicknesses ranging from 50 nm to 1  $\mu\text{m}$ . The morphology of the film surface in contact

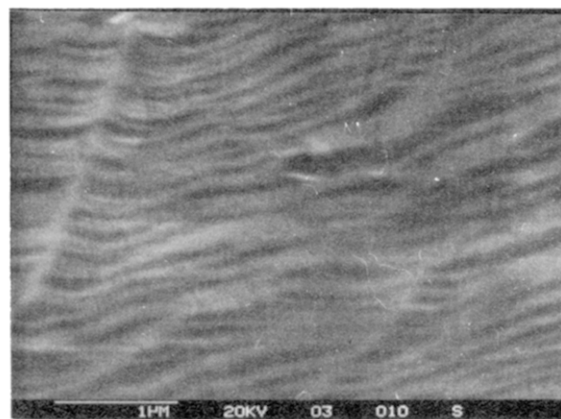


**Figure 2.** SEM picture of the electrode side of a 200-nm-thick PMeT film prepared on a 8-cm<sup>2</sup> platinum plate with the conditions of Figure 1.

with the electrolytic medium appears drastically affected by the increase of film thickness, changing from a smooth compact structure to an increasingly disordered morphology. In contrast, the view of the electrode side of the films (Figure 2) presents a very compact morphology. This picture displays parallel grooves representing the negative print of the mechanical polishing of the platinum surface, which indicates that the polymer covers evenly the anode surface. Furthermore, the similarity of the pictures obtained with various film thicknesses shows that the morphology of the electrode side of the film is independent of the film thickness.

The large dissimilarity between the two sides of the films shows that the morphology of the polymer evolves rapidly from a very compact structure to an increasingly disordered one during electropolymerization. On the basis of these observations, one could expect the polymer formed during the early stages of polymerization to be more ordered and probably more conducting.

**Electrical Conductivity.** The major problem encountered during conductivity measurements resulted from the fragility of ultrathin films, which has limited the extent of our experiments on thicknesses between 0.1 and 1  $\mu\text{m}$ . This point is illustrated by the variation of the conductivity of PMeT films on ITO as a function of their thickness (Figure 3). The conductivity presents a broad maximum for thicknesses around 200 nm, which illustrates the practical limit of the present experimental conditions for the manipulation of ultrathin films. Figure 4 shows the dependence of the conductivity on the current density applied for electrosynthesis for 200-nm-thick PMeT films prepared with 0.2 and 0.1 M monomer. These curves show that for each monomer concentration an optimal current density leading to the highest conductivity can be defined. This optimal current density, which is rather broad for high monomer concentration, decreases and becomes more sharply defined as the monomer concentration is lowered. It is worth noting that in each case, the optimal current density corresponds to a potential of 2.2–2.5 V/SCE, suggesting that for a given monomer concentration, the optimal current density corresponds to an optimal rate of polymer growth.

On ITO electrodes, the highest conductivities ( $1.36 \times 10^3 \text{ S cm}^{-1}$ , Figure 3) are obtained with 0.1 M monomer, lower concentrations leading to brittle films. In contrast, on platinum anodes, a further decrease of monomer concentration down to 0.05 M leads to a further enhancement of the conductivity which reaches values lying in the  $2 \times 10^3 \text{ S cm}^{-1}$  region (Table I). These results show that platinum anodes allow the preparation of more conducting

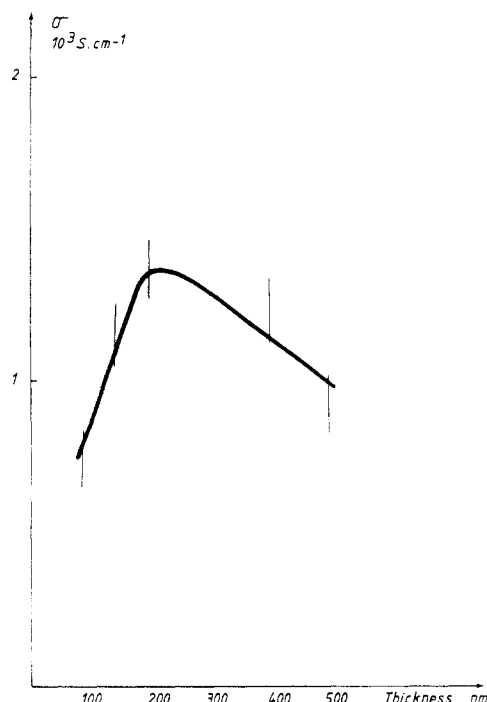


**Figure 3.** Effect of film thickness on the conductivity of PMeT films prepared on ITO with 0.1 M MeT.

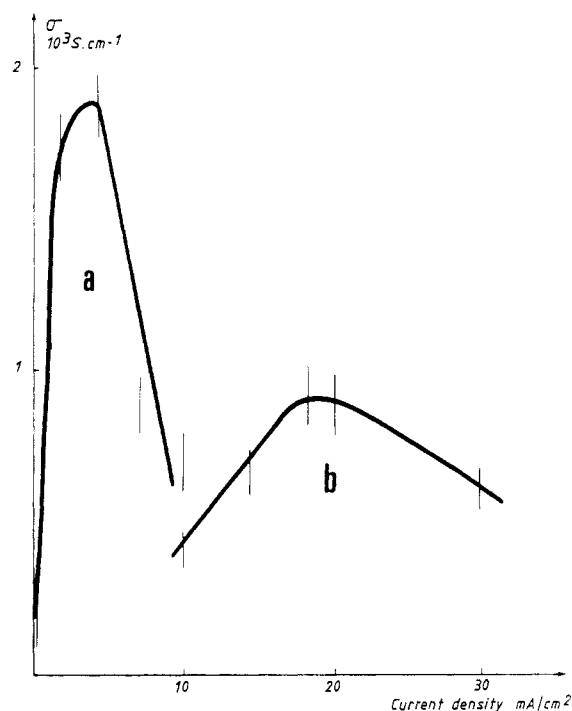


**Figure 4.** Effect of the synthesis current density on the conductivity of 200-nm-thick PMeT films prepared with (a) 0.1 M MeT on Pt and (b) 0.2 M MeT on ITO.

**Table I**  
Conductivities of PMeT Films Prepared on Pt with 0.05 M MeT and 1.5 mA/cm<sup>2</sup>

thickness, nm	10 <sup>3</sup> σ, S cm <sup>-1</sup>	thickness, nm	10 <sup>3</sup> σ, S cm <sup>-1</sup>
380	1.470 ± 0.14	200	1.975 ± 0.19
300	1.540 ± 0.15	140	1.430 ± 0.14
220	1.860 ± 0.18		

thin films with lower monomer concentrations and lower current densities than ITO electrodes.

Hillman et al. have shown recently that the electropolymerization of thiophene is preceded by the adsorption

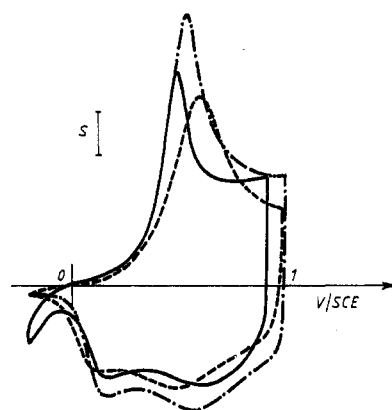


**Figure 5.** Cyclic voltammograms recorded in 0.1 M LiClO<sub>4</sub>/CH<sub>3</sub>CN, for PMeT films prepared on ITO with 0.1 M MeT and 5 mA/cm<sup>2</sup>: (---) film thickness 200 nm, *S* = 100 μA; (- - -) film thickness 50 nm, *S* = 20 μA; (—) film thickness 5 nm, *S* = 2 μA.

of the monomer onto the electrode surface.<sup>11</sup> These authors and others have proposed that the initial step in the electropolymerization consists in the formation of a monolayer of polymer growing bidimensionally, parallel to the electrode surface.<sup>12,13</sup> On the basis of this hypothesis, the differences observed between ITO and platinum anodes could reflect the differences in the efficiency of monomer adsorption as it seems evident that thiophene adsorbs more strongly on platinum than on ITO. Such an interpretation appears consistent with the results of previous works in which we have shown that on ITO surface, the initial potential is the determining factor controlling the density of initial nucleation sites and hence the cohesion and the conductivity of the resulting films.<sup>14</sup> Moreover, this interpretation is consistent with the strong effect of the electrode resistivity on the spectroscopic properties of PMeT that will be discussed in a following section.

The highest conductivity obtained here was about  $2 \times 10^3$  S cm<sup>-1</sup>. Although 4 times larger than the highest values reported so far,<sup>6</sup> this result still represents a lower limit, and it is highly probable that the conductivity of thinner films should be much higher. Theoretical conductivity values of  $(1.5\text{--}2) \times 10^3$  S cm<sup>-1</sup>, based on the Drude approximation<sup>15</sup> or on data extrapolated from short chain oligomers,<sup>16</sup> have been already proposed for polythiophenes. While in light of the present results these last values are clearly underestimated, our results appear consistent with the value of  $1.3 \times 10^4$  S cm<sup>-1</sup> proposed recently on the basis of electron spin resonance data.<sup>17</sup>

The correlation observed between the morphology and the conductivity of the polymer films suggests that a denser structure, corresponding probably to a more ordered stacking of the polymer chains, is a determining factor for the increase of conductivity observed in thin films. However, another possible cause for these high conductivities can involve modifications of the intramolecular structure of the polymer chains and particularly a longer mean conjugation length in ultrathin films. This eventuality has been considered by analyzing the evolution of the electrochemical and spectroscopic properties of PMeT as a function of film thickness.

**Cyclic Voltammetry.** Figure 5 compares the cyclic voltammograms of PMeT films of 200-, 50-, and 5-nm thickness on ITO. These curves and the data in Table II show that decreasing the thickness of the polymer film leads to a sharpening of the anodic wave, together with a 90-mV shift of the anodic current peak (*E*<sub>p</sub>) toward less positive potentials. These results suggest an improvement of the electrochemical reversibility of the doping/undoping

**Table II**  
Cyclic Voltammetric Data Recorded in 0.1 M  
LiClO<sub>4</sub>/CH<sub>3</sub>CN for PMeT Films Prepared on ITO  
Electrodes with 0.1 M MeT and 5 mA/cm<sup>2</sup> (Scan Rate 10  
mV/s)

thickness, nm	$E_{pa}$ , V/SCE	$E_{pc}$ , V/SCE	$I_{pa}$ , $\mu\text{A}/\text{cm}^2$	$I_{pc}$ , $\mu\text{A}/\text{cm}^2$	$I_{min}/I_{pa}$
6	0.52	0.56	7.4	2.9	0.56
14	0.53	0.56	15.2	5.6	0.55
21	0.54	0.56	23.7	9.9	0.57
54	0.56	0.56	71.4	28.6	0.56
104	0.58	0.55	148	56.8	0.56
190	0.61	0.53	236	104	0.57

**Table III**  
Effects of Film Thickness on the Absorption Maximum of  
Undoped PMeT Films Prepared on SnO<sub>2</sub> with 0.1 M MeT  
and 5 mA/cm<sup>2</sup>

thickness, nm	$\lambda_{max}$ , nm	thickness, nm	$\lambda_{max}$ , nm
190	510	20	530
104	514	11	548
54	516	6	552
50	516		

process as thickness decreases. Such a conclusion is consistent with previous observations reported for polypyrrole<sup>9</sup> and also with the decreasing stability of the doped state observed when rinsing ultrathin films ( $\approx 100$  Å) with acetone.

Diaz et al. have already shown that in the case of pyrrole and thiophene oligomers the oxidation potential determined by cyclic voltammetry and the position of the absorption maximum are tightly correlated to the extent of conjugation.<sup>18</sup> More recently, similar correlations have been observed also in the case of the polymers prepared from thiophene oligomers.<sup>7</sup> As a consequence, the sharpening of the anodic wave and the shift of  $E_p$  toward less positive values observed when reducing the film thickness appear consistent with a narrower distribution of the various lengths of conjugated segments and also with a longer mean conjugation length in thinner films.

However, the interpretation of cyclic voltammetric data of conducting polymers is not straightforward since in addition to the length and distribution of the various conjugated segments in the polymer, the shape of the voltammograms depends on the nature of the ionic species used as dopant<sup>19</sup> and also on the relative contribution of the capacitive charging currents<sup>8,20</sup> with possible interactions between these various parameters. As already shown, the capacitive charging currents appear as current plateaus following the anodic wave in the current-voltage curve.<sup>20</sup> Consequently, a rough estimate of the relative contribution of capacitive currents can be obtained by measuring the ratio of the anodic peak current  $I_{pa}$  to the minimum of current following the anodic wave  $I_{min}$ . As appears in Table II, this ratio is constant throughout the whole range of thicknesses, suggesting that the relative contribution of capacitive currents is independent of film thickness, which support the above interpretation of the evolution of the voltammogram. However, since these results do not constitute unequivocal evidence of such an interpretation, they have been completed by an analysis of the spectroscopic properties of PMeT as a function of film thickness.

**Visible Absorption Spectroscopy.** Figure 6 shows the absorption spectra of undoped PMeT films grown on SnO<sub>2</sub> electrodes as a function of film thickness. These spectra and Table III show that when the thickness is decreased from 200 to 5 nm, the absorption maximum shifts bathochromically from 510 to 552 nm. Such a displacement of the absorption maximum indicates that the average length

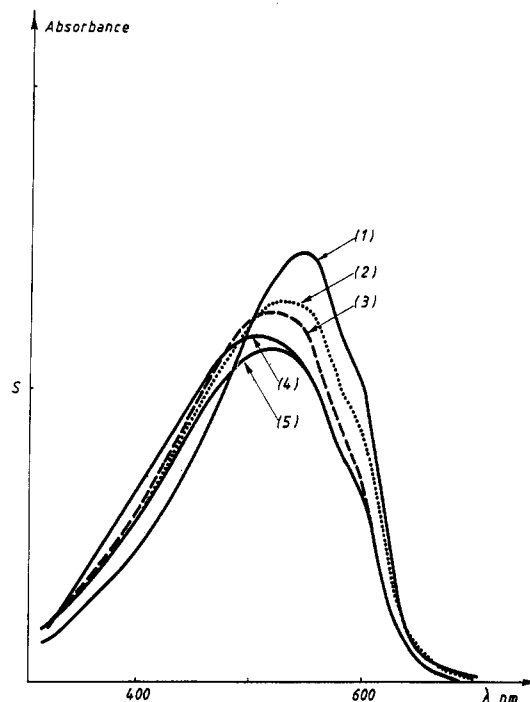


**Figure 6.** UV-vis absorption spectra of undoped PMeT films on SnO<sub>2</sub> electrodes. Film thickness: (1) 6 nm,  $S = 0.05$ ; (2) 20 nm,  $S = 0.25$ ; (3) 50 nm,  $S = 0.5$ ; (4) 104 nm,  $S = 1$ ; (5) 190 nm,  $S = 2$ .

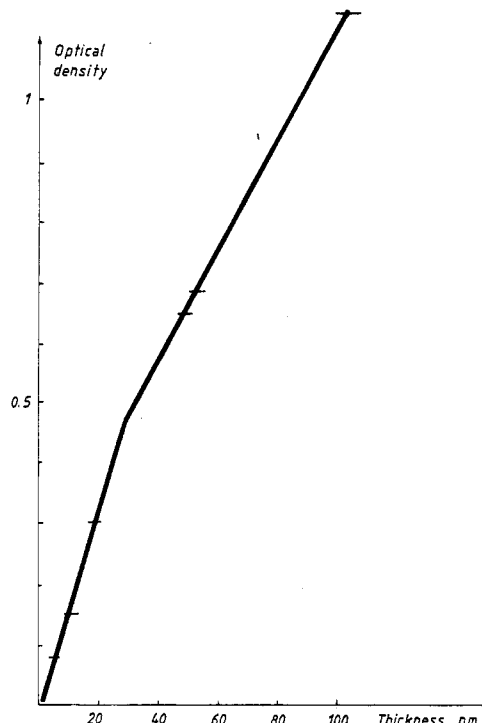


**Figure 7.** Variation of the optical density at  $\lambda_{max}$  vs thickness for undoped PMeT films on SnO<sub>2</sub>.

on which the  $\pi$ -electron delocalization occurs is considerably more extended in thinner films. Furthermore, the narrowing of the width at half-maximum appears consistent with a narrower distribution of the various lengths of conjugated segments already suggested by the electrochemical results.

In a recent communication, a 20-nm shift was obtained for the same range of thickness by using  $80 \Omega \text{ cm}^{-2}$  ITO electrodes.<sup>21</sup> The much larger shift observed on SnO<sub>2</sub> anodes confirms the determining role of the nature of the working electrode on the properties of the polymer, in

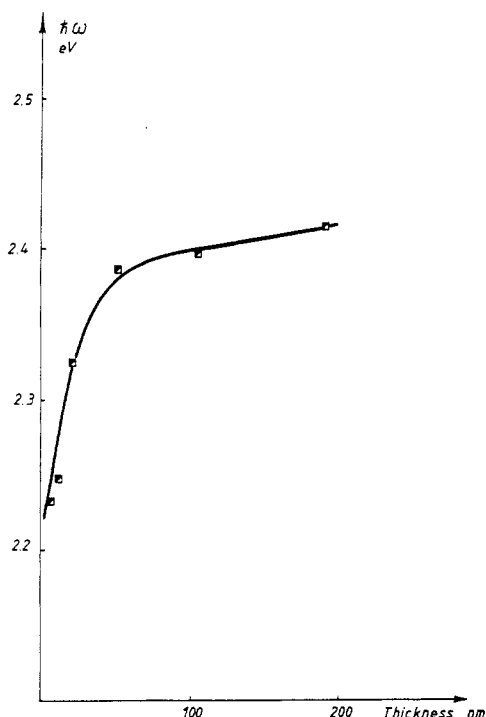


**Figure 8.** Variation of the absorption maximum vs thickness for undoped PMeT films on  $\text{SnO}_2$ .

agreement with the conductivity values.

Figure 7 shows the variation of the optical density at  $\lambda_{\text{max}}$  versus film thickness. Although close to the experimental uncertainty, the slight increase of the slope indicates that the molecular absorption coefficient of the polymer is higher in the thinner films as is generally observed when the conjugation increases.<sup>22</sup> The variation of the absorption maximum of PMeT films as a function of thickness (Figure 8) shows that the largest energy shift occurs between 6 and 20 nm. These results indicate that the mean conjugation length is more extended in very thin films, and that a steep decrease of the mean conjugation length occurs after the growth of a film corresponding to a few monolayers. Since the highest conductivities have been measured on films of 200-nm thickness, the spectroscopic data obtained on ultrathin films strongly suggest that the conductivity of these films should be much larger than the present experimental values.

The conductivity of electrogenerated conducting polymers is the sum of two contributions corresponding respectively to the interchain and the intrachain charge-transport processes. The interchain conductivity depends essentially on the intersegment carrier hopping frequency while the intrachain conduction is determined by the mean conjugation length in the polymeric chains.

The literature offers a different analysis concerning the relative importance of the intrachain and interchain processes. Wegner has suggested that the conjugation length does not play a major role for the final value of conductivity.<sup>23</sup> On the other hand, experimental correlations of the conductivity with the mean conjugation length have been reported for polyacetylene<sup>24</sup> and poly-*p*-phenylene.<sup>25</sup> In the case of polythiophene, correlations have been also observed between the conductivity and the mean conjugation length as determined by Raman spectroscopy,<sup>26</sup> from data obtained on short chains oligomers,<sup>16</sup> or by selective deuterium labeling of the monomer.<sup>27</sup> In fact, a clearcut distinction between the interchain and the intrachain processes is not evident since, as shown by Baughman and Shacklette, both the electronic conduc-

tivity and the intersegment carrier hopping frequency are predicted to increase with the conjugation length.<sup>28</sup>

The mean effective conjugation length along the polymeric chains depends on two parameters; the stereoregularity of the polymer, e.g., the ratio of  $\alpha\text{-}\beta'$ / $\alpha\text{-}\alpha'$  linkages occurring during the polymerization and also the various conformations adopted by stereoregular chains. We have shown already that the mean number of  $\alpha\text{-}\beta'$  couplings occurring during the electropolymerization is largely determined by the monomer concentration and electrical conditions used for the preparation of the film since these two factors control the relative magnitude of the parallel formation of oligomers during the polymerization.<sup>6b,29</sup> Due to the lower ratio of their  $\alpha\text{-}\beta$  reactivity, these oligomers lead to a statistical increase of the number of  $\alpha\text{-}\beta'$  linkages and thus to a decrease of the mean conjugation length.<sup>30</sup> Although of different origins, the two factors determining the effective mean conjugation length are not independent since the occurrence of  $\alpha\text{-}\beta'$  linkages in a given chain modifies the electronic repartition in this chain, which in turn can promote the formation of ramifications on sites rendered more energetically favorable than the polymer chain end. Furthermore, the occurrence of linkage errors in a given chain can generate distortions in adjacent chains and thus perturb the  $\pi$ -electron delocalization in stereoregular chains. It appears thus that a conjugation defect occurring in the very early steps of polymerization will have much more dramatic consequences for the overall stereoregularity and stacking order of the polymer chains grown subsequently than the same defect occurring at a later stage of polymerization.

In summary our results suggest that the high conductivity of very thin films has different origins. A more extended mean conjugation length related to a lower number of linkage errors during the early stages of polymerization, which leads consequently to less distorted conformations in the first layers and thus to a higher intrachain conduction. This higher stereoregularity results in a denser packing arrangement of the polymer chains in very thin films, which minimizes the average interchain distance and hence increases the probability of charge carrier hopping in the case of a three-dimensional variable-range hopping of localized states.<sup>31</sup>

## Conclusion

The properties of PMeT films have been analyzed at various stages of electropolymerization. Under well-controlled electrosynthesis conditions, the conductivity of thin polymer films reaches values up to  $2 \times 10^3 \text{ S cm}^{-1}$ , which are 4 times larger than the value obtained on films of a few micrometers thickness. The large decrease of the conductivity with thickness is correlated with a gradual modification of the morphology toward a more disordered structure. A parallel analysis of the evolution of the electrochemical and spectroscopic properties as a function of film thickness has shown that the mean conjugation length is considerably more extended in ultrathin films. These results imply that both intra- and intermolecular cooperative effects contribute to the rapid increase of the disorder and hence to the decrease of the conductivity as polymerization proceeds.

**Registry No.** PMeT, 84928-92-7.

## References and Notes

- (a) Diaz, A. F.; Kanazawa, K.; Gardini, G. P. *J. Chem. Soc., Chem. Commun.* **1979**, 635. (b) Tourillon, G.; Garnier, F. J. *Electroanal. Chem.* **1982**, 135, 173.
- (a) Heeger, A. J. *Comments Solid State Phys.* **1981**, 10, 53, (b) Brédas, J. L.; Themans, B.; André, J. M.; Chance, R. R.; Silbey, R. *Synth. Met.* **1984**, 9, 265. (c) Harbeke, G.; Meier, E.; Kobel,

- W.; Egli, M.; Kiess, H.; Tosatti, E. *Solid State Commun.* **1985**, *55*, 419. (d) Kaneto, K.; Kohno, Y.; Yoshino, K. *Solid State Commun.* **1984**, *51*, 267.
- (3) (a) Yoshino, K.; Kaneto, K.; Inuishi, Y. *Jpn. J. Appl. Phys.* **1983**, *22*, 3, L157. (b) Tourillon, G.; Garnier, F. *J. Phys. Chem.* **1984**, *88*, 5281. (c) Roncali, J.; Garnier, F. *J. Chem. Soc., Chem. Commun.* **1986**, 783. (d) Lemaire, M.; Delabouglise, D.; Garreau, R.; Roncali, J. *Recent Advances in Electroorganic Synthesis*; Torri, S., Ed.; Elsevier Science: 1987, p 385. (e) Lemaire, M.; Delabouglise, D.; Garreau, R.; Guy, A.; Roncali, J. *J. Chem. Soc., Chem. Commun.* **1988**, 658.
- (4) (a) White, H. S.; Kittlesen, G. P.; Wrighthon, M. S. *J. Am. Chem. Soc.* **1984**, *106*, 5375. (b) Glenis, S.; Tourillon, G.; Garnier, F. *Thin Solid Films* **1984**, *122*, 9.
- (5) (a) Waltman, R. J.; Bargon, J.; Diaz, A. F. *J. Phys. Chem.* **1983**, *87*, 1459. (b) Kaneto, K.; Kohno, Y.; Yoshino, K.; Inuishi, Y. *J. Chem. Soc., Chem. Commun.* **1983**, 282. (c) Hotta, S.; Hosaka, T.; Shimotsuma, W. *Synth. Met.* **1983**, *6*, 69.
- (6) (a) Sata, M.; Tanaka, S.; Kaeriyama, K. *Synth. Met.* **1986**, *14*, 279. (b) Roncali, J.; Garnier, F. *New J. Chem.* **1986**, *10*, 237.
- (7) Roncali, J.; Garnier, F.; Lemaire, M.; Garreau, R. *Synth. Met.* **1986**, *15*, 323.
- (8) Roncali, J.; Garreau, R.; Yassar, A.; Marque, P.; Garnier, F.; Lemaire, M. *J. Phys. Chem.* **1987**, *91*, 6706.
- (9) (a) Mohammadi, A.; Inganäs, O.; Lundström, I. *J. Electrochem. Soc.* **1986**, *133*, 5, 947. (b) Osaka, T.; Naoi, K.; Ogano, S.; Nakamura, S. *Chem. Lett.* **1986**, 1687. (c) Hahn, S. J.; Stanchina, W. E.; Gadjia, W. J.; Vogelhut, P. *J. Electron. Mater.* **1986**, *15* (3), 145.
- (10) Tourillon, G.; Garnier, F. *J. Polym. Sci.* **1984**, *22*, 33.
- (11) Christensen, P. A.; Hamnett, A.; Hillman, A. R. *J. Electroanal. Chem.* **1988**, *242*, 47.
- (12) Hillman, A. R.; Mallen, E. *J. Electroanal. Chem.* **1987**, *220*, 351.
- (13) Tourillon, G.; Dartyge, E.; Fontaine, A.; Garrettt, R.; Sagurton, M.; Xu, P.; Williams, G. P. *Europhys. Lett.* **1987**, *4*, 12, 1391.
- (14) Roncali, J.; Garnier, F. *J. Phys. Chem.* **1988**, *92*, 833.
- (15) Tourillon, G.; Garnier, F. *J. Phys. Chem.* **1983**, *87*, 2289.
- (16) Cao, Y.; Guo, D.; Pang, M.; Qian, R. *Synth. Met.* **1987**, *18*, 189.
- (17) Schärli, M.; Kiess, H.; Harbecke, G.; Berlinger, W.; Blazey, K. W.; Müller, K. A. *Synth. Met.* **1988**, *22*, 317.
- (18) Diaz, A. F.; Crowley, J.; Bargon, J.; Gardini, G. P.; Torrance, J. B. *J. Electroanal. Chem.* **1981**, *121*, 355.
- (19) (a) Diaz, A. F.; Castillo, J. I.; Logan, J. A.; Lee, W. Y. *J. Electroanal. Chem.* **1981**, *129*, 115. (b) Marque, P.; Roncali, J.; Garnier, F. *J. Electroanal. Chem.* **1987**, *218*, 107.
- (20) (a) Feldberg, S. W. *J. Am. Chem. Soc.* **1984**, *106*, 4671. (b) Tanguy, J.; Mermilliod, N.; Hoclet, M. *J. Electrochem. Soc.* **1987**, *134*, 795.
- (21) Roncali, J.; Yassar, A.; Garnier, F. *J. Chem. Soc., Chem. Commun.* **1988**, 581.
- (22) (a) Jaffé, H. H.; Orchin, M. *Theory and Applications of Ultraviolet Spectroscopy*; Wiley: New-York, 1966; p 228. (b) Sease, J. W.; Zechmeister, L. *J. Am. Chem. Soc.* **1947**, *69*, 270.
- (23) Wegner, G. *Makromol. Chem. Makromol. Symp.* **1986**, *1*, 151.
- (24) Soga, K.; Nakamaru, M. *J. Chem. Soc., Chem. Commun.* **1983**, 1495.
- (25) Havinga, E. E.; Van Horssen, L. W. *Synth. Met.* **1986**, *16*, 55.
- (26) Furukawa, Y.; Akimoto, M.; Harada, I. *Synth. Met.* **1987**, *18*, 151.
- (27) Delabouglise, D.; Garreau, R.; Lemaire, M.; Roncali, J. *New J. Chem.* **1988**, *12*, 155.
- (28) Baughman, R. H.; Shacklette, L. W. *Synth. Met.* **1987**, *17*, 173.
- (29) Roncali, J.; Lemaire, M.; Garreau, R.; Garnier, F. *Synth. Met.* **1987**, *18*, 139.
- (30) Waltman, R. J.; Bargon, J. *Can. J. Chem.* **1986**, *64*, 76.
- (31) (a) Kanazawa, K. K.; Diaz, A. F.; Gill, W. D.; Grant, P. M.; Street, G. B.; Gardini, G. P. *Synth. Met.* **1979/80**, *1*, 329. (b) Tanaka, M.; Watanabe, A.; Fujimoto, H.; Tanaka, J. *Mol. Cryst. Liq. Cryst.* **1982**, *83*, 277.

## Dynamic-Mechanical Properties and Cross-Polarized, Proton-Enhanced, Magic Angle Spinning $^{13}\text{C}$ NMR Time Constants of Poly[oligo(ethylene glycol) dimethacrylates]

P. E. M. Allen,\*† G. P. Simon,‡ D. R. G. Williams,§ and E. H. Williams§

Departments of Physical and Inorganic Chemistry and Chemical Engineering, The University of Adelaide, G.P.O. Box 498, Adelaide, SA 5001, Australia.

Received April 4, 1988; Revised Manuscript Received August 2, 1988

**ABSTRACT:** Dynamic-mechanical and fracture properties and proton-enhanced, magic angle spinning  $^{13}\text{C}$  NMR time constants for polymers of the  $\text{CH}_2=\text{C}(\text{CH}_3)\text{CO}(\text{OCH}_2\text{CH}_2)_x\text{OCOC}(\text{CH}_3)=\text{CH}_2$  series ( $x = 1$  to  $\bar{x} = 22$ ) and poly[tetrakis(ethylene glycol) diacrylate] have been measured. The effects of increasing length of the soft oxyethylene chain,  $x$ , undercure ( $x = 1-4$ ), and oxyethylene crystallization ( $\bar{x} = 22$ ) were observed. The results are interpreted in terms of the contributions of components of group motion to the cooperative motion of segments of the network which control the response to a macroscopic deformation.

### Introduction

We present the results of dynamic-mechanical and fracture tests on glycol dimethacrylate networks prepared from a homologous series of monomers:  $\text{CH}_2=\text{C}(\text{CH}_3)\text{CO}(\text{OCH}_2\text{CH}_2)_x\text{OCOC}(\text{CH}_3)=\text{CH}_2$ . In the series the soft oxyethylene chains were cross-linked by hard methacrylate links. The increasing length,  $x$ , of the oxyethylene link is a measure of  $M_c$ , the molecular weight between cross-links. We have varied this from  $x = 1$  in poly(ethylene glycol dimethacrylate) (PEGDMA) to a number-average  $\bar{x} = 22$  in P1000EGDMA.

The increasing flexibility of the network was due to both the decrease in cross-link density and the dilution of stiff methacrylate chains by flexible oxyethylene links. The

trend was opposed by the onset of crystallization of the oxyethylene chain in P1000EGDMA and by the diminishing effects of residual monomer at ultimate cure in the glassy samples from PEGDMA to PTetEGDMA (poly[tetrakis(ethylene glycol) dimethacrylate]). Cross-polarized, proton-enhanced, magic angle spinning (CP/PE/MAS)  $^{13}\text{C}$  NMR was applied to measure the unsaturation at ultimate cure and estimate the proportions that corresponded to free monomer. The PE/MAS  $^{13}\text{C}$  NMR time constants  $T_{\text{SL}}$  and  $T_{1\rho}(\text{C})$  were also measured. These parameters are sensitive to molecular motion at and around the C-atoms responsible for the NMR line under observation.

### Experimental Section

**Materials.** Ethylene glycol dimethacrylate (EGDMA), tris- and tetrakis(ethylene glycol) dimethacrylates (TriEGDMA and TetEGDMA), and tetrakis(ethylene glycol) diacrylate (TetEGDA) were obtained from Fluka. Bis(ethylene glycol) dimethacrylate

\* Department of Physical and Inorganic Chemistry.

† Now at Adran Gemeg, Coleg Prifysgol, Aberystwyth, UK.

‡ Now at Varian Associates Inc., Palo Alto, CA.

§ Department of Chemical Engineering.